# MODELING TRANSIENT TEMPERATURE DISTRIBUTIONS AROUND LANDMINES IN HOMOGENOUS BARE SOILS

J. Simunek
George E. Brown Jr. Salinity Laboratory, Riverside CA 92507
jsimunek@ussl.ars.usda.gov

J.M.H. Hendrickx and B. Borchers
New Mexico Tech, Socorro NM 87801
hendrick@nmt.edu



## ABSTRACT

The objective of this study is to expand our exploration of the effects of the soil environment on landmine detection by investigating the influence of soil texture and water content on surface soil temperatures above antitank mines buried at 15 cm depth and away from it. Temperature distributions in July were calculated in six soil textures (sandy loam, loam, silt, silt loam, sandy clay loam, and clay loam) for the climatic conditions of Kuwait and Sarajevo. We evaluated the temperature distributions in typical dry and wet soil profiles. The simulated temperature differences varied from .22-.63 degree Celcius in Kuwait to .16-.37 in Sarajevo. Temperature differences were –with one exception– larger in the wet than in the dry soils which suggests that soil watering may help improve thermal signatures. A major finding of this study is that the thermal signature of an anti tank mine strongly depends on the complex interaction between soil texture, water content, and geographical location. It is very difficult to predict the exact time or even the approximate hour of the appearance or nonappearance of a thermal signature. Therefore, this modeling study indicates that the use of a thermal sensor in a real mine field for instantaneous mine detection carries a high risk. On the other hand if a given area can be monitored constantly with a thermal sensor for twelve hours or longer the thermal signature will be detected if the signal to noise ratio of the mine environment allows so. Field experiments are needed to validate the results of this modeling study.

**Keywords**: soil temperature, modeling, Kuwait, Bosnia, soil type, climate, antitank mine.

## 1. INTRODUCTION

Many sensors for landmine detection are affected by the water content, temperature, electrical conductivity and dielectric constant of the surrounding soil. The most important of these is soil water content since it directly influences the three other properties. Das et al.[1] and Hendrickx et al.[2] have studied transient soil water content regimes around landmines in six soil textures varying from sandy loam to clay loam under the climatic conditions of humid Bosnia and arid Kuwait. Their results indicate that soil water distributions around landmines can be highly variable in space and time. Occasional short-term accumulation or loss of soil water around landmines depends greatly on soil type and weather conditions. Water movements to and from shallow soil depths are driven by precipitation events and the evaporative demand of the atmosphere. The process is so dynamic in time that an analytical steady-state approach is not appropriate for the assessment of soil water distributions around landmines.

Soil water content determines to a large extend the electrical and thermal soil properties. Borchers et al.[3] assessed in which manner the changes in electrical soil properties caused by water content changes affect the velocity and attenuation of radar signals as well as the strength of radar reflection from landmines. Under dry weather conditions water contents at shallow soil depths frequently will be too low for good radar performance. However, artificial soil watering or heavy precipitation events that wet the soil to water contents exceeding 20 volume percent improve soil conditions for optimal performance of ground penetrating radar systems in sand and loam soils. The objective of this study is to expand our exploration of the effects of the soil environment on landmine detection by investigating the influence of soil texture and water content on surface soil temperatures above antitank mines and away from it.

Detection and Remediation Technologies for Mines and Minelike Targets VI, Abinash C. Dubey, James F. Harvey, J. Thomas Broach, Vivian George, Editors, Proceedings of SPIE Vol. 4394
(2001) © 2001 SPIE · 0277-786X/01/$15.00

## 2. HEAT FLOW IN SOILS

### 2.1 Heat Flow Equation

Neglecting the effects of water vapor diffusion, two-dimensional heat transport can be described as[4]

$$C\frac{\partial T}{\partial t}=\frac{\partial}{\partial x_i}\left[\lambda_{ij}\frac{\partial T}{\partial x_j}\right]-C_w q_i\frac{\partial T}{\partial x} \tag{1}$$

where $T$ is temperature [K], $t$ is time [T], $x$ is distance [L], $q$ is water flux [$LT^{-1}$], $\lambda_{ij}$ is the apparent thermal conductivity of the soil [$MLT^{-3}K^{-1}$] (e.g. $Wm^{-1}K^{-1}$) and $C$ and $C_w$ are the volumetric heat capacities [$ML^{-1}T^{-2}K^{-1}$] (e.g. $Jm^{-3}K^{-1}$) of the soil and the soil water phase, respectively. Volumetric heat capacity is defined as the product of the bulk density and gravimetric heat capacity. The first term on the right-hand side of Equation (1) represents heat flow due to conduction and the second term accounts for heat being transported by flowing water. In this study we do not consider the transfer of heat by flowing water nor the transfer of latent heat by vapor movement. We also make the common assumption that the apparent thermal conductivity does not depend on the direction of the heat flow. Therefore, Equation (1) simplifies to

$$C\frac{\partial T}{\partial t}=\lambda\left[\frac{\partial^2 T}{\partial x^2}+\frac{\partial^2 T}{\partial z^2}\right] \tag{2}$$

where $z$ is depth [L]. According to de Vries[5] the volumetric heat capacity of a soil $C$ can be expressed as

$$C=C_n\theta_n+C_o\theta_o+C_w\theta_w+C_g\theta_g \tag{3}$$

where $\theta$ refers to a volumetric fraction [$L^3L^{-3}$], and subscripts $n$, $o$, $w$, $g$ represent the solid phase, organic matter, the liquid phase and gas phase, respectively. The contribution of the gas phase is so small that it can be neglected.

For a given soil the thermal conductivity becomes a function of the volumetric soil water content[6] which can be described as

$$\lambda(\theta)=b_1+b_2\theta_w+b_3\theta_w^{0.5} \tag{4}$$

where $b_1$, $b_2$ and $b_3$ are empirical parameters [$MLT^{-3}K^{-1}$] (e.g. $Wm^{-1}K^{-1}$).

### 2.2 Surface Heat Flux

The daily course of upward or downward heat fluxes through the soil surface can be measured with a "soil heat flux plate" that is located just below the soil surface. The device consists of two thin parallel metal plates with a thermocouple battery between them. The temperature difference between the two plates located perpendicularly to the direction of expected heat flux generates an electric current proportional to the temperature difference which is proportional to the heat flux. Soil heat fluxes can also be calculated from measured soil temperature profiles and soil thermal properties. Since no measured heat fluxes nor temperature profiles were available for this study, an indirect method has been used for the determination of representative daily heat fluxes in Kuwait and Bosnia during the hottest and coldest month of the year, i.e., July and January respectively.

The average daily values of global radiation $R_g$ for Sarajevo (Bosnia, Northern latitude 42°) and Kuwait (Kuwait, Northern latitude 30°) were obtained from the Atlas of World Water Balance[7] and are presented in Table 1.

Table 1. Average daily values of global radiation $R_g$ in Kuwait and Sarajevo during January and July.

| Location | Global Radiation | |
|---|---|---|
| | January | July |
| | W m$^{-2}$ | |
| Kuwait | 232 | 451 |
| Sarajevo | 145 | 460 |

Then, an empirical equation[8] was used to calculate the daily radiation $R_n$ in the hottest (July) and coldest (January) period of the year using the $R_g$

$$R_n = \left(a + b\frac{n}{N}\right) R_g \tag{5}$$

where $a$ and $b$ are empirical constants that depend on the location, the season and the state of the atmosphere, and $n/N$ is the relative duration of sunshine. For a clear sky Equation (5) simplifies to

$$R_n = a' R_g \tag{6}$$

where $a'$ is an empirical constant. The value of this constant depends mainly on the albedo of the soil surface which depends on soil color, soil water content, and soil roughness. We used average values of $a'$ equal to 0.7 for Kuwait and 0.4 for Sarajevo.

The daily heat flux, $G_d$, through the soil surface was then calculated using another empirical equation[8]

$$G_d = c R_n \tag{7}$$

where $G_d$ is the daily average value of the downward heat flux into soil (Wm$^{-2}$), and $c$ is an empirical constant. For a bare soil, Fuchs and Hadas[9] found that, on average, $c$=0.3, but $c$ can have a value anywhere in the range of 0.2 and 0.7. Combining Equations (6) and (7) we approximate the average daily heat flux through the soil surface as

$$G_d = c R_n = c a' R_g = A R_g \tag{8}$$

where $A$ is approximately equal to 0.12 (0.3*0.4) and 0.21 (0.3*0.7) for Sarajevo and Kuwait, respectively.

The distribution of the heat flux during a 24 hour period was derived under the assumption that the heat flux has a sinusoidal shape with symmetric positive and negative fluxes during day and night, respectively. The negative flux (upward into the atmosphere) as well as the positive flux (downward into the soil profile) have a duration of 12 hours with the maximum downward flux occurring at 1 p.m. The net heat flux into the soil profile during the 24 hour period is considered zero so that the equation for soil heat flux becomes

$$G = G_{\max} \sin\left(\frac{2\pi}{t_p} t - \frac{7\pi}{12}\right) \tag{9}$$

where $t_p$ is the period of time necessary to complete one cycle of the sine wave, i.e. 1 day, and $t$ is time in days. The second term within the argument of the sine function is included to allow the highest soil heat flux to occur at 1 p.m. Equation (9) has been used in this study to describe daily variations of the heat flux across the soil surface. The values of the average daily soil heat flux $G_d$ and maximum heat flux $G_{max}$ for Kuwait and Sarajevo during January and July are presented in Table 2.

Table 2. Values of the heat flux parameters at Kuwait and Sarajevo in January and July.

| Location | Heat Fluxes | | | |
|---|---|---|---|---|
| | $W\ m^{-2}$ | | | |
| | January | | July | |
| | $G_d$ | $G_{max}$ | $G_d$ | $G_{max}$ |
| Kuwait | 49 | 77 | 95 | 149 |
| Sarajevo | 17 | 27 | 55 | 86 |

## 3. NUMERICAL MODELING

We have solved numerically the water flow and heat transport equations using the finite element method for the spatial discretization and the finite differences method for the temporal discretization as implemented in the HYDRUS-2D model[10]. Although the HYDRUS-2D model has the capability to simultaneously solve the water flow and heat transport equations we used a more straightforward approach in this study to minimize computer time. We considered soil water content as a static variable and only simulated heat transport. This approach is justified by the fact that under most soil moisture conditions soil water content changes slowly over a period of several days whereas soil temperatures close to the soil surface show a clear daily cycle.

The static soil water content distributions used in this study have been obtained from Das et al.[1] who have evaluated the effects of land mines on water content distributions in six different soil textures under the climatic conditions of Kuwait and Sarajevo. We selected a characteristic dry and wet profile for Kuwait and Sarajevo, respectively, for all six soil textures: silt, clay loam, loam, silt loam, sandy clay loam, sandy loam. The original transport region for water flow calculations consisted of a quasi three-dimensional region exhibiting radial symmetry about a vertical axis. Water flow was simulated in a soil cylinder with a radius of 2 m and depth of 2 m. The antitank mine was placed in the center of the cylinder with its bottom at a depth of 0.23 m. The height of the mine was 0.08 m and its diameter was 0.3 m. Since the area occupied by a landmine was assumed not to be part of the transport domain in water flow calculations, this area was cut out of the computational domain.

Contrary to water flow calculations, the land mine must be a part of the transport domain for heat movement calculations, since heat can freely transfer from soil to a mine, and vice versa. Thus we modified the transport domain by making the area occupied by a landmine a part of the computational domain. Since HYDRUS-2D does not provide an option to keep the original finite element mesh and to include additional regions, we generated a new mesh with 10089 elements for a transport domain that included a landmine and interpolated characteristic dry and wet water content profiles of Das et al.[1] on this new mesh for all six soil textures.

The buried land mine was modeled as a homogeneous block of TNT. Mines are actually much more complex structures, consisting of TNT and the plastic container. But we assumed that the overlying soil blurs the details of the mine's shape and construction, and its overall effects on the temperature profiles.

Empirical parameters $b_1$, $b_2$ and $b_3$ of the thermal conductivity function (Eq. 4) for clay, loam and sand were taken from Chung and Horton[6] and are given in Table 3. Empirical parameters $b_1$, $b_2$ and $b_3$ of the thermal conductivity function were available only for three soil types and they had to be used for all six textural classes. This approach can be justified by the fact that thermal soil properties are much more influenced by water content than by textural differences[11]. The last column of Table 3 gives the association of the thermal conductivity parameters with various textural classes as used in calculations. The thermal properties of TNT are given in Table 4.

Observation nodes were located at six different depths (0, 2.5, 7.5, 11.5, 30, and 37.5 cm) and two different locations (4.0 and 115 cm away from the radial axis) for monitoring soil temperatures. Temperatures at positions close to the radial axis (4.0 cm) were affected by the presence of the land mine while those far from the radial axis (115 cm) were not affected by the land mine.

Table 3. Empirical parameters $b_1$, $b_2$, and $b_3$ of the thermal conductivity function[6].

| | Empirical Parameters | | | |
|---|---|---|---|---|
| Soil Type | $b_1$ | $b_2$ | $b_3$ | Used for Soil Texture |
| Clay | -0.197 | -0.962 | 2.521 | Silt, Clay Loam |
| Loam | 0.243 | 0.393 | 1.534 | Loam, Silt Loam, Sandy Clay Loam |
| Sand | 0.228 | -2.406 | 4.909 | Sandy Loam |

Table 4. Thermal properties of TNT (obtained from US Army Night Vision Laboratory).

| Property | Value |
|---|---|
| Thermal conductivity ($W\ m^{-1}\ K^{-1}$) | 0.234 |
| Volumetric heat capacity ($J\ m^{-3}\ K^{-1}$) | $2.5297\times10^{6}$ |

Temperature distributions in the month of July were calculated for 24 characteristic water content profiles (6 x 2 x 2) subject to a periodic heat flux (Eq. 9) across the soil surface. Six soil textures (sandy loam, loam, silt, silt loam, sandy clay loam, and clay loam), two climatic conditions (Kuwait and Sarajevo), and wet and dry soil profiles were used in particular combinations of computational conditions. Initial calculations were performed for a period of one month. However, since there were no distinguishable differences in temperature profiles in later daily cycles, we carried out calculations for a period of only 5 days.

## 4. RESULTS AND DISCUSSION

### 4.1 Soil Temperature Distributions in Dry and Wet Soils

All temperature distributions in the soils without land mine, i.e. at the observation points located 115 cm away from the radial axis of the simulation domain or 100 cm away from the edge of the land mine, show typical distributions as reported in the literature[5,11]. For example, Figures 1 and 2 present the temperature changes for depths 2.5, 7.5, 11.5, and 37.5 cm in a typical dry and wet loam soil at Kuwait and Sarajevo in July. The daily temperature amplitude is larger in the dry than in the wet soil because of the smaller volumetric heat capacity of dry soil. The daily temperature amplitude decreases with depth and at depth 37.5 cm it becomes less than one degree Celcius. The maximum temperature at depth lags behind the hour of maximum temperature at 2.5 cm depth, the lag time is approximately 12 hours at depth 37.5 cm. Figures 1 and 2 also demonstrate the rather small soil temperature difference between locations above a mine and away from it. The only difference between the soil temperature distributions in Kuwait and Sarajevo is the size of the temperature amplitude which is larger at Kuwait than at Sarajevo as a result of the larger net radiation flux received at this location.

### 4.2 Temperature Effects of Antitank Land Mines

The thermal conductivity of a land mine corresponds approximately to the thermal conductivity of an air-dry soil and therefore is significantly lower than the thermal conductivity of most field soils. The volumetric heat capacity of a land mine is, however, approximately equal to that of a wet soil. Figures 1 and 2 show that in spite of these differences in thermal properties between TNT and field soils, the temperature differences above and away from a land mine buried at 15 cm depth are fairly small. In addition to this the figures also demonstrate that the daily heat wave hardly penetrates to a depth of 30 cm. Therefore, a strong temperature response at the soil surface would not be expected.

Figure 1. Temperatures in the observation nodes at depths 2.5, 7.5, 11.5, and 37.5 cm in a typical dry and wet loam soil at Kuwait in July. The dotted line represents temperatures away from the mine and the solid line temperatures above and below the mine. The largest temperature amplitude is observed at 2.5 cm, the smallest one at 37.5 cm.

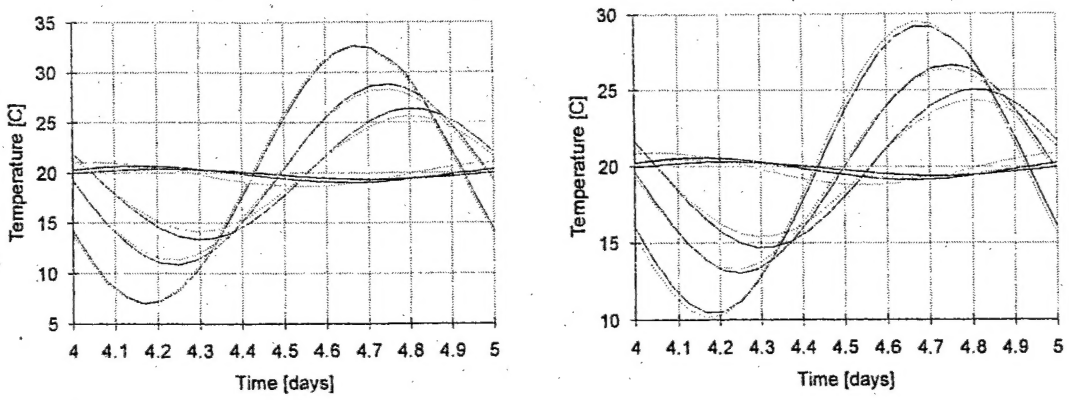


Dry Loam Soil

Wet Loam Soil

Figure 2. Temperatures in the observation nodes at depths 2.5, 7.5, 11.5, and 37.5 cm in a typical dry and wet loam soil at Sarajevo in July. The dotted line represents temperatures away from the mine and the solid line temperatures above and below the mine. The largest temperature amplitude is observed at 2.5 cm, the smallest one at 37.5 cm.

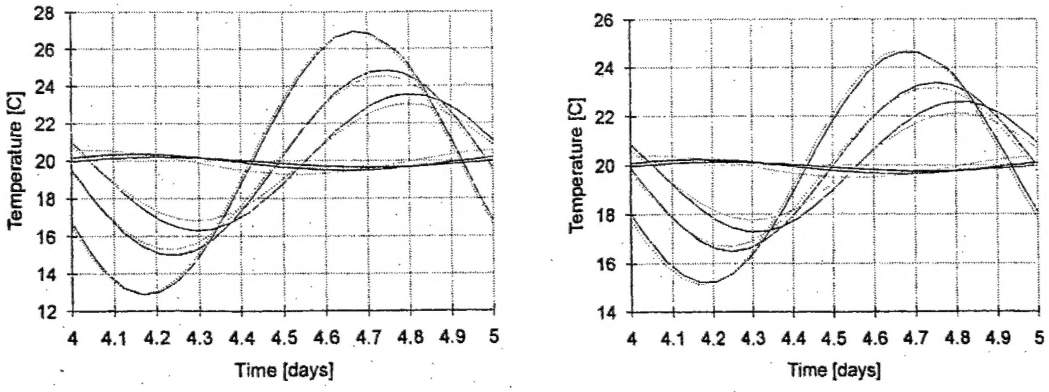


Dry loam soil

Wet loam soil

We also examined the temperature differences at the soil surface above the mine and away from it. Table 5 presents maximum temperature differences for all soil textures at Kuwait and Sarajevo in July. A wet soil –with one exception in the sandy loam at Sarajevo– leads to a larger temperature difference than a dry soil. This suggests that soil watering may improve temperature differences. If this hypothesis derived from this modeling study can be confirmed in experimental studies, it would be an important finding since in sand soils watering does also improve radar signatures[3]. Two sensors that both perform better after soil watering could considerably enhance the results of sensor fusion.

The complexity of the thermal processes that produce the temperature signatures can be appreciated by studying the temperature differences for the two soils with the lowest and highest maximum differences at Kuwait and Sarajevo, respectively (Figures 3 and 4). The smallest temperature differences were found in a dry clay loam at Kuwait and Sarajevo. However, at Kuwait the largest difference was found in the wet sand loam while at Sarajevo it was found in the dry sand loam. In Kuwait, the temperature differences during a 24 hour period are almost identical in a wet clay loam and in a dry sand loam while these soils behave completely different in Sarajevo. This means that it will be very difficult to quantify temperature differences, i.e. thermal signatures, in real mine fields.

Figures 3 and 4 also show that the time of day at which the largest temperature difference occurs, depends in a complex manner on soil texture and water content as well as geographical location, i.e. the soil heat flux. All maximum temperature differences occur around 12:00 am or 12:00 pm plus or minus three hours. For example, the maximum differences in a wet sand loam at Kuwait occur at approximately 9:00 am and at 9:00 pm. However, the smallest difference of zero, i.e. the complete absence of thermal signature, occurs at 3:00 pm and 3:00 am which falls within the six hour period in which the strongest thermal signature is expected to appear. On the other hand, in the *dry* sand loam at Kuwait the strongest thermal signature occurs at approximately 3:00 pm and 3:00 am (Figure 3). Apparently, a change of soil water content can have a strong effect on the timing of the thermal signatures. Obviously, such complex thermal behavior will cause severe problems when thermal sensors are used in real mine fields since there appears no easy way to predict optimal hours for mine detection. Field calibration in the mine field is also cumbersome since relatively small changes of soil water content may result in large shifts in the appearance of thermal signatures.

Table 5. Maximum temperature differences (°C) simulated during July in Kuwait and Sarajevo in six soil textures under dry and wet soil moisture conditions.

| Soil Texture | Soil Moisture | Maximum Temperature Difference (°C) | |
|---|---|---|---|
| | | Kuwait | Sarajevo |
| Clay Loam | Dry | 0.22 | 0.16 |
| | Wet | 0.49 | 0.18 |
| Loam | Dry | 0.35 | 0.21 |
| | Wet | 0.58 | 0.25 |
| Silt Clay Loam | Dry | 0.35 | 0.23 |
| | Wet | 0.56 | 0.26 |
| Silt | Dry | 0.29 | 0.21 |
| | Wet | 0.39 | 0.19 |
| Silt Loam | Dry | 0.37 | 0.27 |
| | Wet | 0.53 | 0.24 |
| Sand Loam | Dry | 0.53 | 0.37 |
| | Wet | 0.63 | 0.35 |

Figure 3. The temperature difference between the soil surface immediately above the anti tank mine and away from the mine in Kuwait during two days in July in a clay loam and in a sand loam soil under wet and dry conditions.

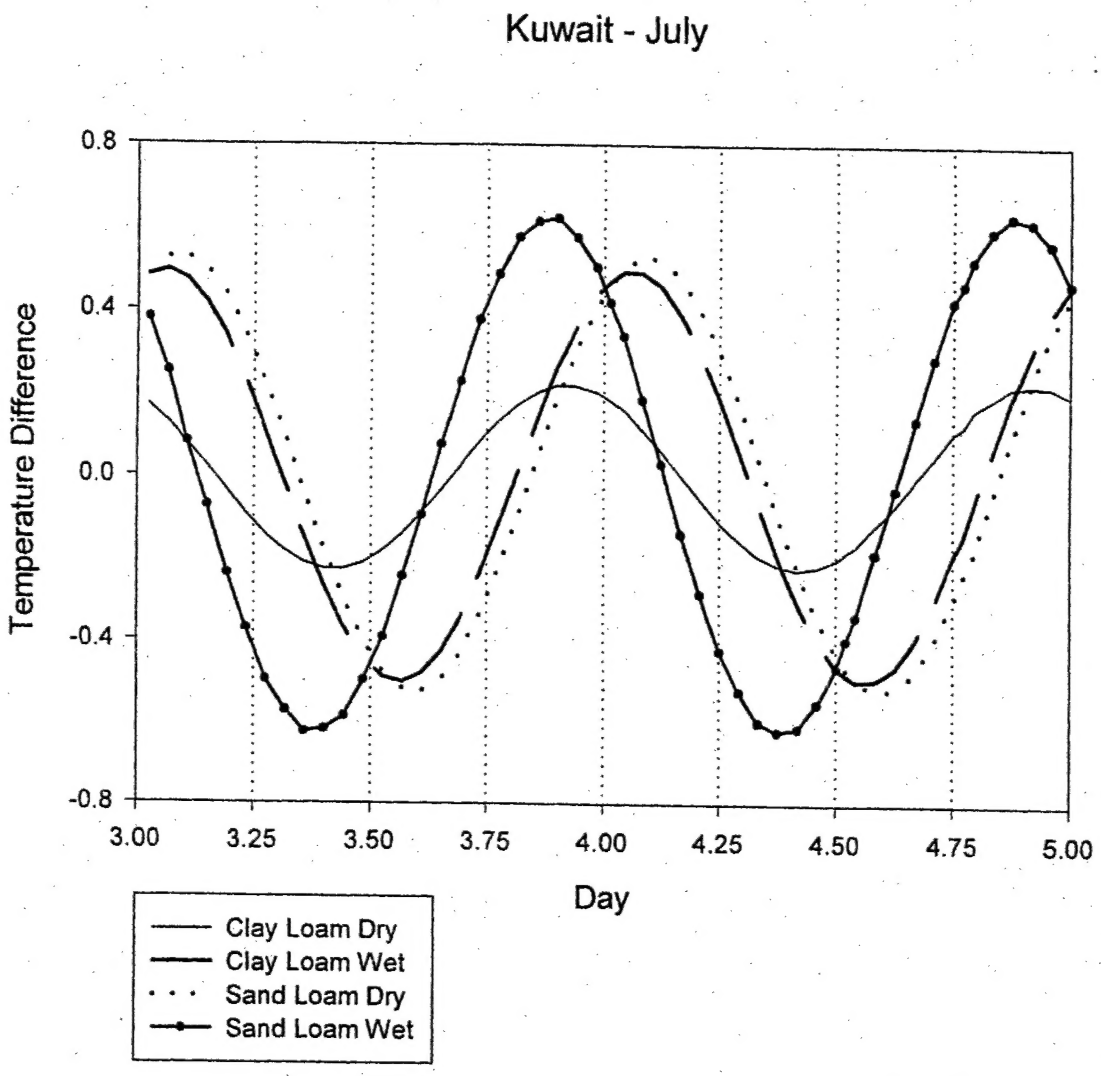

Figure 4. The temperature difference between the soil surface immediately above the anti tank mine and away from the mine in Sarajevo during two days in July in a clay loam and in a sand loam soil under wet and dry conditions.

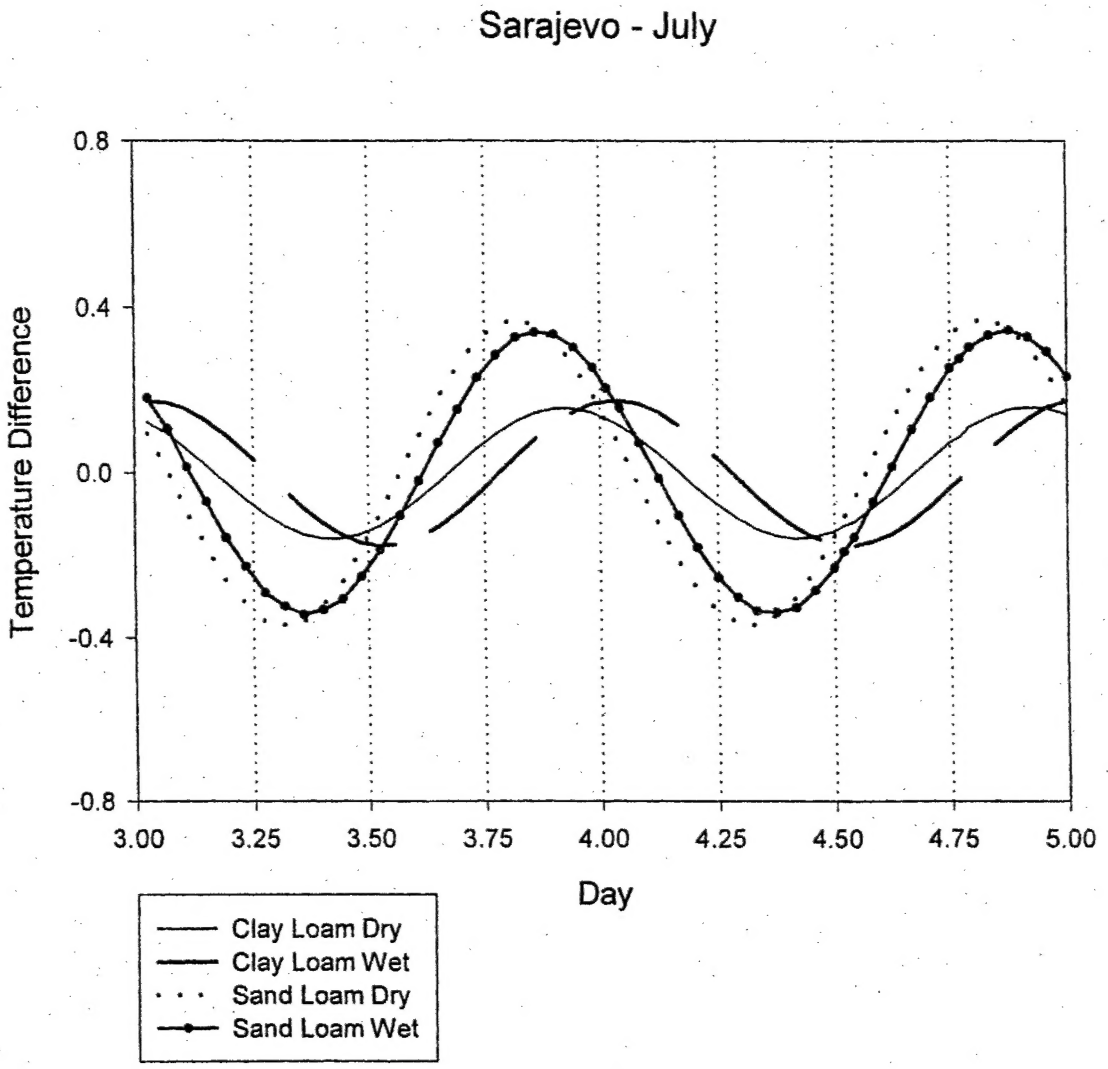

## 5. CONCLUSIONS

A major finding of this study is that the maximum temperature difference between the soil surface above the mine and areas away from it, i.e. the strongest thermal signature, depends in a complex manner on the thermal properties of the soil, i.e. soil texture and soil water content, as well as the soil heat flux, i.e. geographical location and time of the year.

The strongest thermal signature seems to appear in two six hour intervals centered around 12:00 am and 12:00 pm but its exact time is very difficult to predict. To make matters worse, the weakest thermal signatures frequently can also be found in these time intervals. Therefore, this modeling study indicates that the use of a thermal sensor in a real mine field for instantaneous mine detection carries a high risk. On the other hand if a given area can be monitored constantly with a thermal sensor for twelve hours or longer the thermal signature will be detected if the signal to noise ratio of the mine environment allows so. Field experiments are needed to validate the results of this modeling study.

In this simulation study it was determined that the temperature signature of buried land mines is slightly more pronounced in wet than in dry soils. More research will be conducted to explore whether this finding will hold for mines buried at shallower and deeper depths.

## ACKNOWLEDGEMENT

This work is funded by a grant from the Army Research Office (Project 38830-EL-LMD). The authors would like to thank Dr. Russell S. Harmon, Senior Program Manager at the Army Research Office, for his valuable advice and support.

## REFERENCES

1. Das, B.S., J.M.H. Hendrickx, and B. Borchers. 2001. Modeling transient water distributions around landmines in bare soils. *Soil Science* vol. 166, in press.

2. Hendrickx, J.M.H., B.S. Das, and B. Borchers. 1999. Modeling distributions of water and dielectric constants around landmines in homogeneous soils. *Proc. of SPIE* Vol. 3710, *Detection and Remediation Technologies for Mines and Minelike Targets IV*, p. 728-738.

3. Borchers, B., J.M.H. Hendrickx, B.S. Das, and S. Hong. 2000. Enhancing dielectric contrast between land mines and the soil environment by watering: modeling, design, and experimental results. *Proc. of SPIE - The International Society for Optical Engineering (SPIE)*. Vol. 4038 (2):993-1000.

4. Sophocleous, M. 1979. Analysis of water and heat flow in unsaturated-saturated porous media, *Water Resour. Res., 15*(5), 1195-1206.

5. de Vries, D. A. 1963. The thermal properties of soils, In *Physics of Plant Environment*, edited by R. W. van Wijk, pp. 210-235, North Holland, Amsterdam.

6. Chung S.-O., and R. Horton. 1987. Soil heat and water flow with a partial surface mulch, *Water Resour. Res., 23*(12), 2175-2186.

7. Atlas of World Water Balance. 1974. Hydrometeorological Publishing House, Moscow.

8. Brutsaert, W. 1982. *Evaporation into the Atmosphere. Theory, History, and Applications*, D. Reidel Publishing Company, Dordrecht, Holland.

9. Fuchs, M. and A. Hadas. 1972. The heat flux density in a non-homogeneous base loessial soil, *Boundary-Layer Meteorol. 3*, 191-200.

10. Simůnek, J., M. 'ejna, and M. Th. van Genuchten. 1999. The HYDRUS-2D software package for simulating two-

dimensional movement of water, heat, and multiple solutes in variably saturated media. Version 2.0, *IGWMC - TPS - 53,* International Ground Water Modeling Center, Colorado School of Mines, Golden, Colorado, 251pp.

11. Jury, W.A., W.R. Gardner and W.H. Gardner. 1991. *Soil Physics. Fifth Edition*, John Wiley & Sons, New York, NY.